Journal of Stress Analysis
Vol. 9, No. 1, 2025, 119-133
Bu-Ali Sina University

ORIGINAL RESEARCH PAPER

Finite Element Analysis and Optimization of Composite Patch Repairs for Crack Growth Mitigation in Damaged Composite Sheets

Hamid Mozafari*
Department of Mechanical Engineering, Faculty of Engineering, Payame Noor University, Tehran, Iran.

Article info

Article history:
Received 13 July 2024
Received in revised form
22 June 2025
Accepted 26 June 2025

Keywords:
Finite Element Analysis (FEA)
Crack growth mitigation
Composite patch connection
Multi-objective optimization
Imperialist Competitive Algorithm (ICA)

Abstract

This paper examines the effectiveness of composite patch repairs in mitigating crack growth in damaged composite sheets subjected to tensile loading. Three configurations were analyzed using finite element modeling: an unrepaired sheet, a sheet repaired with a one-sided composite patch, and a sheet repaired with a symmetric two-sided patch. The investigation focuses on how patch material selection influences stress distribution, crack-tip strain, and the overall structural performance of the repaired sheets. To enhance repair efficiency, a multi-objective optimization framework was developed to determine the optimal design of a multilayer composite patch with minimum weight and cost while achieving maximum load-bearing capacity. Two optimization algorithms-the Genetic Algorithm (GA) and the Imperialist Competitive Algorithm (ICA)-were implemented and compared. The results indicate that the symmetric two-sided patch configuration provides the most significant reduction in crack growth and the greatest improvement in structural strength. Moreover, the optimization outcomes show that the ICA outperforms the GA in identifying superior design parameters for composite patch repair. These findings offer insights into crack behavior in composite structures and contribute to the development of lightweight, cost-effective, and high-performance repair strategies for engineering applications.

Nomenclature

GA	Genetic Algorithm	FEA	Finite Element Analysis
ICA	Imperialist Competitive Algorithm	SIFs	Stress Intensity Factors
i, j	tensor indices	SERR	Strain Energy Release Rate
S_c	Critical crack length	ACO	Ant Colony Optimization
X_c	Compressive strength in direction 1	CLT	Classical Laminate Theory
X_t	Tensile strength in direction 1	G	Material-dependent constant
Y_t	Tensile strength in direction 2	ΔK	Range of the stress intensity factor
Y_c	Compressive strength in direction 2	N	Number of load cycles
O	Stress	S	Crack length
F_i, F_{ij}	Strength tensors of the second and fourth order	Δo	Stress range

*Corresponding author: H. Mozafari (Assistant Professor)
E-mail address: mozafari.h@pnu.ac.ir
10.22084/jrstan.2025.29603.1259
ISSN: 2588-2597

z	Coordinate through the thickness of the plate	h	Total thickness of multi-layered composite plate
M	Weight of the sheet	a, b	Length and width of the sheet
ρ_n	Density of the nth layer	t_n	Thickness of the nth layer
CEP	Graphite-Epoxy	BEP	Boron-Epoxy
GEP	Glass-Epoxy	EP	Epoxy
Al	Aluminum	E	Yong Modulus
A_{ij}	Elements of the in-plane stiffness matrix	N_f	Number of remaining cycles to failure
B_{ij}	Elements of the coupling stiffness matrix	D_{ij}	Elements of the bending stiffness matrix
N_x, N_y, N_z	Force resultant in the X, Y and Z direction	M_x, M_y, M_z	Moment resultant about the X, Y and Z axis

1. Introduction

Composite materials are widely used in aerospace, automotive, marine, and structural applications due to their high strength-to-weight ratio, corrosion resistance, and design flexibility [1- 2]. Despite these advantages, composite components are susceptible to various forms of damage, including matrix cracking, delamination, and fiber breakage. Among these, crack initiation and propagation represent critical failure mechanisms that can significantly reduce structural integrity and service life. In many engineering systems, damaged composite panels cannot be easily replaced due to cost, accessibility, or the need to maintain continuous operation. Consequently, the development of effective repair techniques for restoring structural performance has become a vital area of research.

Composite patch repair has emerged as one of the most efficient and practical methods for repairing damaged composite structures. The technique involves bonding a composite patch-typically a fiber-reinforced polymer laminate-over the damaged region to redistribute stresses, arrest crack propagation, and restore load-carrying capacity. Compared to traditional repair methods such as bolted or riveted metallic patches, composite patches offer several advantages, including reduced weight, minimal stress concentrations, improved fatigue resistance, and better compatibility with the repaired substrate. As a result, composite patch repair is increasingly adopted in modern engineering applications where lightweight and high-performance repairs are essential [3].

Subsequent studies focused on improving patch efficiency by tailoring patch materials, geometry, and thickness. Researchers have shown that both single-sided and double-sided patch configurations can effectively reduce stress intensity at the crack tip, with symmetric double-sided patches offering enhanced structural balance and reduced bending effects. In particular, two-sided repairs have been found to significantly decrease out-of-plane deformation and interlaminar stresses, contributing to more uniform load transfer [4-5].

The advantages of using composite patches for repair are numerous. Firstly, the composite materials can increase the strength of the repaired structure without the need for drilling or riveting, which can compromise structural integrity. Additionally, composite patches offer a weight-efficient solution compared to traditional metal-based repair methods, as they can provide enhanced strength-to-weight ratios. The flexibility in designing and arranging the composite layers also allows for the repair of irregularly shaped components, which is a significant benefit in many engineering applications [6].

Moreover, composite materials exhibit excellent fatigue and corrosion resistance, making them well-suited for applications in which the repaired structure is subjected to cyclic loads or harsh environmental conditions. Finally, the use of composite patch repairs can result in cost savings by reducing the need for extensive component replacement or complex machining operations. It is important to note, however, that the installation time and process complexity associated with composite patch repairs should also be considered when evaluating the suitability of this approach for a particular application [7- 9].

To design an effective composite patch repair, it is crucial to understand the mechanical behavior of the cracked structure and the repaired system. Finite element analysis (FEA) provides a powerful tool for accurately modeling crack behavior, stress distribution, and the interaction between the patch and the damaged substrate. Numerous studies have applied FEA to evaluate different patch configurations, adhesive properties, and loading conditions. However, determining the optimal patch design-one that maximizes structural performance while minimizing cost and weight-remains a challenging multi-objective problem. Traditional design approaches often rely on trial-and-error or parametric studies, which may not identify the most efficient repair solution [10- 11].

Numerous studies have utilized FEA to model stress distribution, crack-tip fields, and adhesive layer behavior. For example, researchers have employed two-dimensional and three-dimensional FE models to

examine how patch stiffness, adhesive thickness, and patch shape influence the reduction of stress intensity factors (SIFs). The adoption of fracture mechanics parameters, such as the strain energy release rate (SERR) and J-integral, has enabled more precise characterization of crack behavior in patched composites [12- 13].

To address this challenge, optimization algorithms have been increasingly integrated with FEA-based evaluation. Among various algorithms, evolutionary and population-based techniques such as the Genetic Algorithm (GA) and the Imperialist Competitive Algorithm (ICA) have shown strong capability in handling nonlinear, multi-parameter engineering problems. These algorithms are well suited for exploring complex design spaces and identifying optimal repair configurations that balance competing objectives [14- 15].

In this study, finite element analysis is combined with optimization techniques to investigate the behavior of cracked composite sheets repaired using composite patches. Three scenarios are examined: an unrepaired sheet, a sheet repaired with a single-sided patch, and a sheet repaired with a symmetric two-sided patch. The influence of patch material selection on stress distribution, crack-tip strain, and overall structural performance is evaluated. Additionally, a multi-objective optimization framework is implemented using GA and ICA to design a multilayer composite patch with minimal weight and cost and maximum load-carrying capacity.

Genetic Algorithms (GA) have been among the most commonly used tools in optimizing composite structures due to their robustness in handling nonlinear and multi-dimensional design spaces. Several studies have applied GA to optimize patch thickness, material selection, and stacking sequence. However, GA can be prone to premature convergence and may require significant computational effort, especially when integrated with FEA.

The Imperialist Competitive Algorithm (ICA), inspired by socio-political competition, has emerged as a promising alternative due to its strong exploration capabilities and improved convergence behavior. Although fewer studies have applied ICA specifically to composite patch repair, its documented effectiveness in structural optimization suggests substantial potential for improving repair design efficiency.

Despite the extensive research on composite patch repairs and finite element modeling, notable gaps remain. For example, comparative optimization studies are limited, particularly those evaluating different evolutionary algorithms for patch design. Few studies incorporate multi-objective optimization, simultaneously addressing weight, cost, and structural performance. Also, analyses comparing single-sided and two-sided patch configurations using integrated FEA-optimization frameworks are scarce. Optimization-driven insights into crack growth mitigation for damaged composite sheets are still underdeveloped. Therefore, there is a clear need for a comprehensive investigation that combines finite element analysis with advanced optimization techniques to identify effective, lightweight, and cost-efficient composite patch repair configurations.

The results of this research provide valuable insights into crack mitigation in composite structures and highlight the advantages of using optimization techniques in the design of efficient, lightweight, and cost-effective composite patch repairs. These findings can support engineers in developing improved repair solutions for a wide range of industrial applications.

2. Formulation of the Problem

2.1. Biaxial Failure in Orthotropic Materials

The stress distribution within the layers of an orthotropic material is evaluated using the Tsai–Wu failure criterion. This tensor-based approach predicts the onset of failure by examining the interaction of stresses within each layer. When the criterion indicates that a layer has failed, that layer is excluded from the remaining laminate configuration, thereby reducing the effective number of layers in the composite structure [16]. The Tsai–Wu failure criterion is mathematically expressed as:

$$F_i\sigma_i + F_{ij}\sigma_i\sigma_j = 1 \tag{1}$$

where i and j denote the tensor indices, and F_i and F_{ij} represent the second- and fourth-order strength tensors, respectively. If we consider:

$$\sigma_6 = \tau_{12}\,,\ \sigma_5 = \tau_{31}\,,\ \sigma_4 = \tau_{23} \tag{2}$$

Then, the corresponding expression for a plane-stress condition becomes:

$$F_1\sigma_1 + F_2\sigma_2 + F_6\sigma_6 + F_{11}\sigma_1^2 + F_{22}\sigma_2^2 + F_{66}\sigma_6^2 + 2F_{12}\sigma_1\sigma_2 = 1 \tag{3}$$

The Tsai–Wu failure coefficients F_i and F_{ij} can be related to the principal strength properties of the material, specifically its tensile and compressive strengths along the three orthogonal axes. For the special case in which the applied stresses act along the principal material direction 1, the Tsai–Wu coefficients can be written as:

$$\begin{aligned} &F_1X_t + F_{11}X_t^2 = 1 \\ &F_1X_C + F_{11}X_C^2 = 1 \\ &F_1 = \tfrac{1}{X_t} + \tfrac{1}{X_C} \quad , \quad F_{11} = -\tfrac{1}{X_tX_C} \end{aligned} \tag{4}$$

where X_t is the tensile strength in direction 1, and X_c is the compressive strength in direction 1. In case where the stresses are applied in the principal direction 2, the Tsai-Wu failure coefficients can be expressed as:

$$F_2 = \frac{1}{Y_t} + \frac{1}{Y_C} \quad , \quad F_{22} = -\frac{1}{Y_tY_C} \tag{5}$$

where Y_t is the tensile strength in direction 2, and Y_c is the compressive strength in direction 2. This formulation allows the Tsai-Wu failure criterion to be tailored to the specific strength properties of the orthotropic composite material in the principal direction 2. By considering both the tension and compression states, the model can accurately capture the asymmetric behavior of the material under different loading conditions. The ability to define the Tsai-Wu coefficients using the principal strength values is crucial for the reliable assessment of failure in orthotropic composites, as it enables the direct incorporation of the material's anisotropic characteristics into the failure analysis. In the shear mode, the following relations hold:

$$F_6 = 0 \quad , \quad F_{66} = \frac{1}{S^2} \tag{6}$$

To determine F_{12}, a biaxial stress state must be imposed in which the two principal stresses are applied simultaneously while all other stress components are set to zero.

$$\sigma_1 = \sigma_2 = \sigma(F_1 + F_2)\sigma + (F_{11} + F_{22} + 2F_{12})\sigma^2 = 1 \tag{7}$$

For the Tsai–Wu coefficient F_{12}, which characterizes the interaction between the principal stresses, an expression can be derived using the previously established relationships. The resulting formula for F_{12}, is:

$$F_{12} = \frac{1}{2\sigma^2}\left[1 - \left(\frac{1}{X_t} + \frac{1}{X_C} + \frac{1}{Y_t} + \frac{1}{Y_C}\right)\sigma + \left(\frac{1}{X_t X_C} + \frac{1}{Y_t Y_C}\right)\sigma^2\right] \tag{8}$$

This expression incorporates the tensile and compressive strengths in the two principal material directions (X_t, X_c, Y_t, Y_c) to account for the coupling effects between stresses in an orthotropic material. Including *F12* in the Tsai–Wu failure criterion is essential, as it enables accurate representation of the interaction between principal stresses-an important factor in composite materials, where failure behavior is strongly influenced by multiaxial loading. By adopting this formulation for F_{12}, the Tsai-Wu criterion becomes a more comprehensive and reliable tool for predicting failure initiation in orthotropic composite structures subjected to complex stress states. This enhanced predictive capability is critical for the robust design and analysis of advanced composite materials and components.

2.1.1. Multi-Layer Forces and Moments

In a multilayer composite plate, the resultant forces and moments are obtained by integrating the stresses through the thickness of each individual layer. This procedure yields the total in-plane force and bending moment resultants acting on the plate. The mathematical forms of these resultants are expressed as:

$$\begin{Bmatrix} \mathrm{N_x} \\ \mathrm{N_y} \\ \mathrm{N_{xy}} \end{Bmatrix} = \int_{-t/2}^{t/2} \begin{Bmatrix} \sigma_\mathrm{x} \\ \sigma_\mathrm{y} \\ \tau_\mathrm{xy} \end{Bmatrix} \mathrm{dz} \tag{9}$$

$$\begin{Bmatrix} \mathrm{M_x} \\ \mathrm{M_y} \\ \mathrm{M_{xy}} \end{Bmatrix} = \int_{-t/2}^{t/2} \begin{Bmatrix} \sigma_\mathrm{x} \\ \sigma_\mathrm{y} \\ \tau_\mathrm{xy} \end{Bmatrix} \mathrm{zdz} \tag{10}$$

where N_x, N_γ, and N_z denote the force resultants in the X, Y, and Z directions, and M_x, M_γ, and M_z represent the corresponding moment resultants about the X, Y, and Z axes. The variable z is the coordinate measured through the plate's thickness, and h is the total thickness of the multilayer composite, as illustrated in Fig. 2. Fig. 1 shows the global forces and moments acting on a flat multilayer plate.

By performing these integrations, the contributions of all layers-each with its own anisotropic and heterogeneous properties-are combined to determine the overall force and moment resultants experienced by the composite plate. This information is essential for structural analysis and design, enabling the evaluation of load-bearing capacity and the identification of possible failure mechanisms in multilayer composite structures.

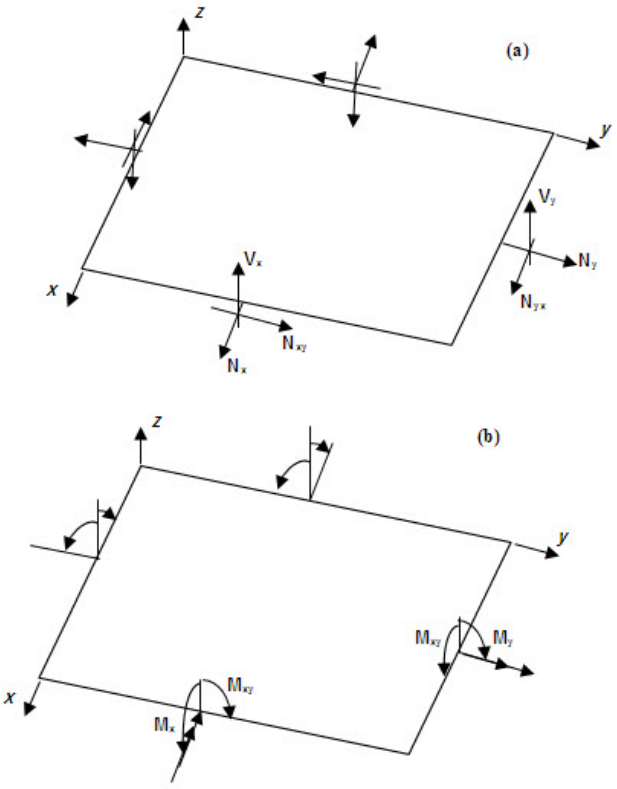

Fig. 1. Forces and moments in a flat multilayer composite plate.

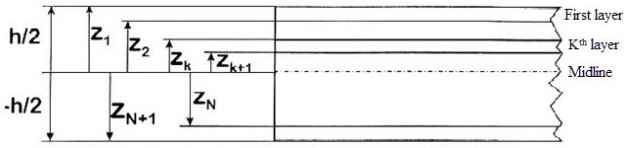

Fig. 2. Layer configuration of the sample composite plate.

The force and moment resultants introduced in the previous equations can be compactly expressed as:

$$\begin{Bmatrix} N_x \\ N_y \\ N_{xy} \\ M_x \\ M_y \\ M_{xy} \end{Bmatrix} = \begin{bmatrix} A_{11} & A_{12} & A_{16} & B_{11} & B_{12} & B_{16} \\ A_{12} & A_{22} & A_{26} & B_{12} & B_{22} & B_{26} \\ A_{16} & A_{26} & A_{66} & B_{16} & B_{26} & B_{66} \\ B_{11} & B_{12} & B_{16} & D_{11} & D_{12} & D_{16} \\ B_{12} & B_{22} & B_{26} & D_{12} & D_{22} & D_{26} \\ B_{16} & B_{26} & B_{66} & D_{16} & D_{26} & D_{66} \end{bmatrix} \begin{Bmatrix} \varepsilon^0{}_x \\ \varepsilon^0{}_y \\ \gamma^0{}_{xy} \\ \kappa_x \\ \kappa_y \\ \kappa_{xy} \end{Bmatrix} \tag{11}$$

$$\begin{aligned} A_{ij} &= \sum_{k=1}^{N} \left(\overline{Q}_{ij}\right)_k \left(z_k - z_{k-1}\right) \\ B_{ij} &= \frac{1}{2} \sum_{k=1}^{N} \left(\overline{Q}_{ij}\right)_k \left(z^2{}_k - z^2{}_{k-1}\right) \\ D_{ij} &= \frac{1}{3} \sum_{k=1}^{N} \left(\overline{Q}_{ij}\right)_k \left(z^3{}_k - z^3{}_{k-1}\right) \end{aligned} \tag{12}$$

In these expressions, A_{ij} denotes the elements of the in-plane (tensile) stiffness matrix, B_j represents the elements of the coupling stiffness matrix-capturing the interaction between in-plane stretching and bending- and D_j corresponds to the elements of the bending stiffness matrix, which governs the flexural response of the multilayer composite plate. Collectively, these matrices (A_j, B_j, and D_j) form the stiffness parameters of Classical Laminate Theory (CLT), which are fundamental to the analysis and design of laminated composite structures.

The A_j matrix characterizes the in-plane load-carrying capacity, the B_j matrix accounts for coupling effects between stretching and bending, and the D_j matrix defines the resistance of the plate to bending loads. Together, they describe the overall mechanical behavior of a multilayer composite plate under various loading conditions.

2.2. Crack Growth Rate Analysis

The Paris law is widely used to evaluate crack growth under fatigue loading. This empirical relation links the crack growth rate to the cyclic stress intensity factor. The Paris law is expressed as:

$$\frac{ds}{dN} = G\Delta K^j \tag{13}$$

In this equation, G and j are material-specific constants determined experimentally, while ΔK denotes the stress intensity factor range-the difference between the maximum and minimum stress intensity factors within a fatigue cycle.

Fig. 3 presents a schematic illustration of the relationship between the crack growth rate and the stress intensity factor in the Paris law model, along with its correspondence to the linear distance from the crack center.

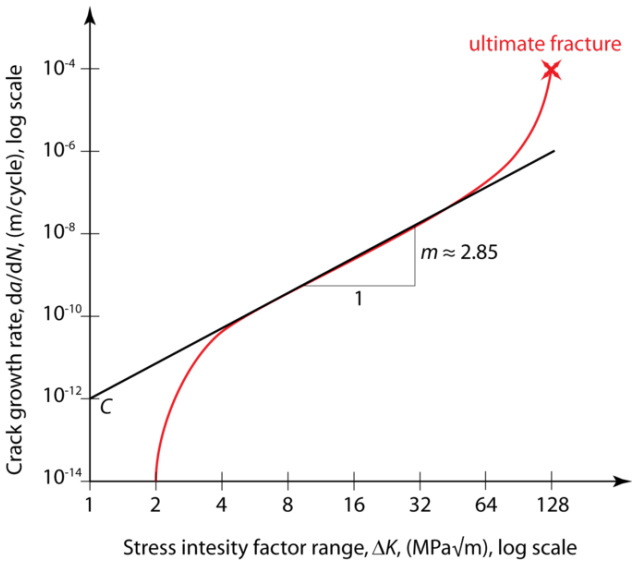

Fig. 3. Schematic diagram showing the relationship between crack growth rate and stress intensity factor in the Paris law model.

In the crack growth equation, s denotes the crack length and N represents the number of loading cycles. The left-hand side, ds/dN, describes the crack growth rate, indicating the infinitesimal increase in crack length per cycle. The stress intensity factor range, ΔK, is calculated using:

$$\Delta K = \Delta\sigma Y\sqrt{\pi s} \tag{14}$$

where Y is a dimensionless geometry factor dependent on the component and crack configuration, σ is the applied stress range, and S is the crack length. For relatively short cracks, Y may be assumed independent of S. Under this assumption, the crack growth equation can be solved by separating variables:

$$\begin{aligned} \int_0^{N_f} dN &= \int_{s_i}^{s_c} \frac{ds}{G\left(\Delta s Y\sqrt{ps}\right)^j} \\ &= \frac{1}{G\left(\Delta s Y\sqrt{p}\right)^j} \int_{s_i}^{s_c} s^{-\frac{j}{2}} ds \end{aligned} \tag{15}$$

Integrating this expression leads to:

$$N_f = \frac{2\left(s^{\frac{2-j}{2}} - s_i^{\frac{2-j}{2}}\right)}{(2-j)\,G\left(\Delta s Y\sqrt{p}\right)^j} \tag{16}$$

Here, N_f is the number of remaining cycles to failure, S_c is the critical crack length at which catastrophic failure occurs, S_i is the initial crack length at the onset of fatigue crack growth, $\Delta\sigma$ is the stress range, and Y is a geometry-dependent constant typically between 0 and 1, based on the initial crack size S_i.

The Paris law is widely used in fracture mechanics to predict crack propagation and estimate the remaining fatigue life of structural components. By applying this relationship, engineers can assess crack growth rates and develop maintenance or replacement strategies that ensure the continued safety and integrity of the structure.

2.3. Imperialist Competition Algorithm

In computer science, the Imperialist Competitive Algorithm (ICA) is a metaheuristic optimization method designed to tackle complex optimization problems. Similar to other nature-inspired algorithms, ICA does not rely on gradient information, making it suitable for nonlinear, discontinuous, or multimodal search spaces. Nature-inspired optimization techniques have proven to be powerful complements to classical mathematical approaches. Well-known examples include Genetic Algorithms (GA), derived from biological evolution, and Ant Colony Optimization (ACO), modeled after the foraging behavior of ants.

ICA draws inspiration from the socio-political dynamics of imperialism, simulating how powerful empires create colonies, compete with rival imperialists, and eventually dominate or lose power through competitive processes. Since its introduction in the early 2000s, ICA has been successfully applied across a wide range of optimization problems, demonstrating its effectiveness and versatility as a global search strategy [17- 18].

The key steps of the Imperialist Competitive Algorithm (ICA) include initializing a population of countries (candidate solutions), forming colonies around the strongest countries (elite solutions), and allowing these colonial powers to compete for greater influence. Over successive iterations, this competitive process drives the system toward the most dominant empire, representing the global optimal solution.

During the algorithm's execution, the weakest colony of the weakest imperialist is reassigned to another empire. The probability of a colony joining a particular imperialist is proportional to that imperialist's relative power. If an imperialist loses all of its colonies, it is eliminated and itself becomes a colony of a more powerful empire. This process is illustrated in Fig. 4.

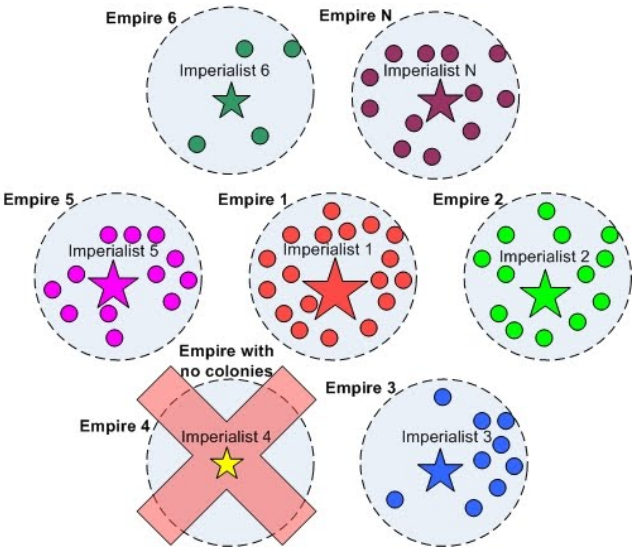

Fig. 4. Schematic representation of imperialist elimination during iterations of the Imperialist Competitive Algorithm.

In this section, three objectives are considered for optimizing composite plates: minimizing weight, minimizing cost, and maximizing the final load capacity. The weight of the plate can be calculated using:

$$M = a.b(\rho_1 t_1 + \rho_2 t_2 + \cdots + \rho_n t_n) \tag{17}$$

where M denotes the total weight of the plate, a and b are its length and width, ρ_n is the density of the n^{th} layer, and t_n is the corresponding layer thickness.

The total cost of the plate depends on two components: the material cost of each layer and the manufacturing cost associated with fiber orientation, as different fiber directions typically incur different production expenses. Let the composite material cost be C_c and the manufacturing cost be C_m. The total cost C_t can then be written as:

$$\begin{aligned} C_c &= \sum_{k=1}^{n} C_{fk} \\ C_m &= \sum_{k=1}^{n} C_{fk} \\ C_t &= C_c + C_m \end{aligned} \tag{18}$$

where C_f represents the cost of each individual layer.

The ultimate breaking load is obtained through numerical analysis, with the failure of the final remaining layer taken as the failure criterion. In this study, the load is applied in the N_x direction of the composite plate. The objective function for the breaking load in the N_x direction is formulated using the global failure criterion:

$$\varphi_3 = \left(2\frac{N_x}{N_x^*}\right)^2 \tag{19}$$

Here, N_x^* represents a predefined maximum load value that remains constant across all models. Accordingly, the final optimization problem is expressed as the unconstrained multi-objective function shown below:

$$f = \varphi_1 + \varphi_2 + \varphi_3 \tag{20}$$

The objective function f is employed to optimize weight, cost, and final load. The functions φ_1 and φ_2 are defined as follows [19]:

$$\varphi_1 = \left(1 + \frac{M}{M^*}\right)^2 \tag{21}$$

$$\varphi_2 = \left(1 + \frac{C}{C^*}\right)^2 \tag{22}$$

In the above relationships, M and C represent the weight and cost of each model, while M^* and C^* denote their corresponding maximum values, which are identical across all designs. As the weight and cost decrease, the normalized values of these terms also decrease, aligning with the optimization goals of this study.

The design variables to be determined for optimizing the objective function include the thickness, fiber orientation angle, and material type of each layer. In this work, a four-layer composite plate is considered, with allowable ranges for fiber angles and layer thicknesses defined as:

$$\begin{aligned} &-90 \le \theta \le 90 \\ &\theta \in \{0, \pm 15, \pm 30, \pm 45, \pm 60, \pm 75, 90\} \\ &0.075 \le t \le 0.3 \\ &t \in \{0.075, 0.1, 0.125, 0.15, 0.175, 0.2, 0.225, 0.25, \\ &\qquad 0.275, 0.3\} \end{aligned} \tag{23}$$

The fiber angles and layer thicknesses are not arbitrary; instead, they follow industry-standard values to ensure manufacturability and structural reliability. Each layer is constructed using these standard specifications. Furthermore, the composite plate is modeled as a hybrid laminate, meaning each layer may be composed of a different material. In this study, three materials-CEP, GEP, and BEP-are selected for evaluation. The mechanical and physical properties of these materials are listed in Table 1.

3. Modeling

3.1. Geometric Characteristics of Samples

This study focuses on evaluating damage in a composite sheet-specifically the presence of a crack-to determine an optimal repair strategy. The composite sheet examined is a rectangular panel produced by Allobond Company, with original dimensions of 1216mm×608mm. It consists of a thermoplastic polyethylene core sandwiched between two aluminum face sheets. As illustrated in Fig. 5, the layers are bonded chemically, mechanically, and thermally, resulting in a lightweight, high-strength composite with a smooth surface and excellent flexibility.

Table 1
Cost values for different angles.

θ	C	θ	C
0	0.035	±60	0.039
±15	0.0375	±75	0.036
±30	0.0395	90	0.0355
±45	0.04		

For the purposes of this analysis, the sheet's length and width have been proportionally scaled down. The total thickness of the composite sheet is 4.2mm, comprising a 3mm polyethylene core, two 0.5mm aluminum layers, and a 0.1mm adhesive layer.

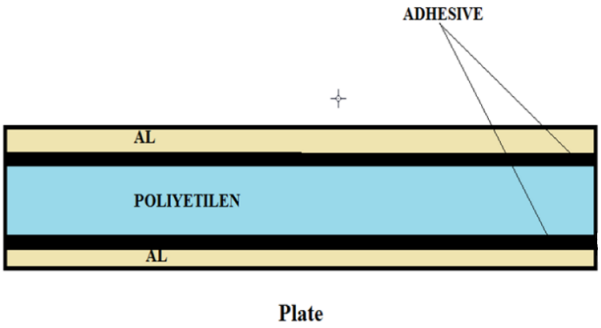

Fig. 5. Materials composing the sample composite sheet.

In this study, the three-dimensional finite element method (FEM) is employed using Abaqus software to model and analyze a cracked composite plate and its corresponding repair patch. For the cracked plate and its components, 8-node solid elements (C3D8R) are used. The same 8-node C3D8R solid elements are applied to model the solid regions of the various composite repair patches, while S4R shell elements are used for components modeled as shell structures.

The final mesh consists of 35,383 elements and 39,312 nodes, with a locally refined mesh around the crack region to improve accuracy. A linear elastic analysis is performed to obtain the output parameters with higher precision. A crack measuring 76mm in length is introduced at the midpoint of one edge of the composite sheet. Tensile loading is applied to the sheet and incrementally increased up to a maximum stress of 100MPa. Fig. 6 illustrates the crack geometry and the corresponding mesh distribution on the composite plate.

This loading configuration is designed to represent realistic service conditions in which the composite sheet may be subjected to mechanical stresses during operation.

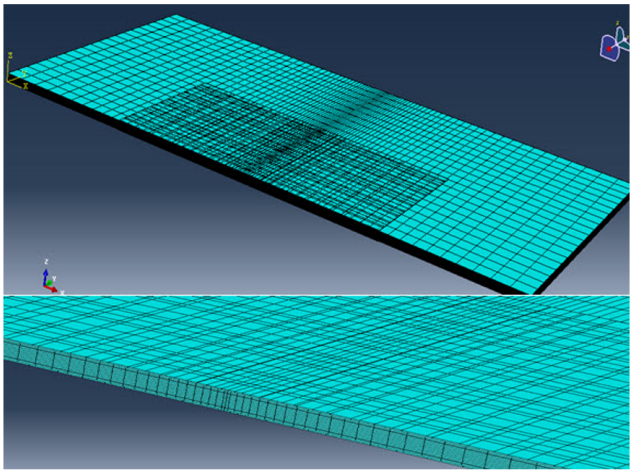

Fig. 6. View of the mesh in the sample composite sheet.

For the repair process, a rectangular composite patch (shown in Fig. 7) is applied to one side of the structure directly over the crack. The patch dimensions are H_{patch}=152mm and W_{patch}=76mm. It consists of four symmetric layers, each 0.15mm thick, with fiber orientations of [0°/90°/90°/0°]. Three composite materials-GEP, BEP, and CEP-are used separately to fabricate the patch samples.

The performance of each patch material is evaluated and compared in terms of mechanical behavior, durability, and crack-repair effectiveness. This comparison helps identify the most suitable material for the repair, considering factors such as strength, weight, and cost-efficiency. The use of a multilayer composite patch with tailored fiber orientations is expected to improve load-bearing capacity and crack-arresting performance relative to single-layer or randomly oriented patches.

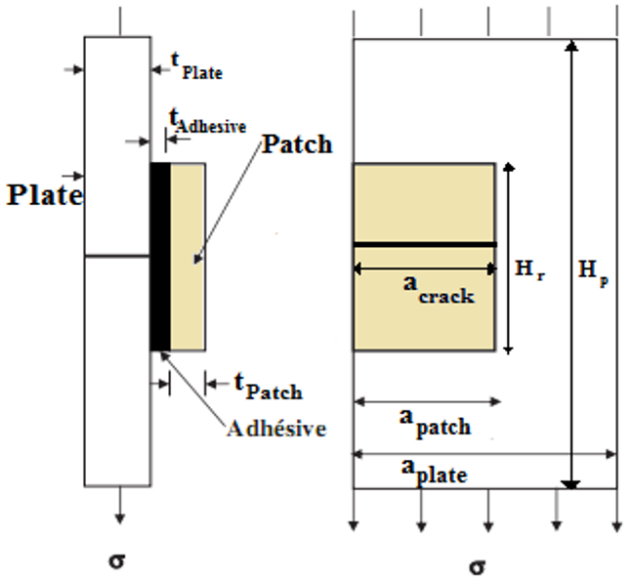

Fig. 7. One-sided composite patch used for repair.

The analysis of the three composite materials provides valuable insight into selecting the optimal patch configuration for the intended repair application.

For the repair process, a rectangular composite patch (Fig. 8) is applied symmetrically over the crack. The patch dimensions are H_{patch}=152mm and W_{patch}=76mm.

The composite patch consists of four symmetric layers, each 0.15mm thick, with fiber orientations of [0°/90°/90°/0°]. Three composite materials-GEP, BEP, and CEP-will be used separately to fabricate the initial patch samples.

In the optimization phase of the study, additional patch configurations will be investigated using GAICA optimization techniques. The optimized patches will also comprise four layers, but each layer may use any combination of the three materials (BEP, GEP, CEP), with fiber orientations ranging from -90° to 90°. The layer thicknesses will be allowed to vary between 0.1mm and 0.3mm. The goal of the optimization is to determine the best material sequence, fiber orientations, and layer thicknesses to maximize load-bearing capacity, improve crack-arrest performance, and enhance the overall effectiveness of the composite repair.

The results from the optimized designs will be compared with the initial three material-based patches to identify the most effective configuration for the repair application.

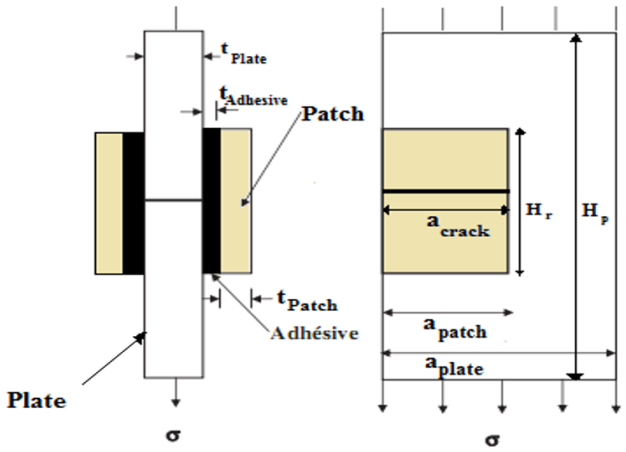

Fig. 8. Two-sided composite patch used for repair.

3.2. Material Specifications

The material specifications for the composite sheet and the repair patches used in this study were provided by the manufacturer, Alupond. The composite sheet serves as the primary structural material, while the epoxy-based composite patches are commonly employed for repair and reinforcement applications. Table 2 presents detailed specifications for both the sample composite sheet and the composite patches used in this research.

The specifications for the composite sheet include information on material composition, physical properties, and performance characteristics. Likewise, the patch specifications detail the material composition, layer dimensions, and other relevant parameters for the epoxy-based repair patches.

A thorough understanding of the material properties of both the composite sheet and the patches is essential for evaluating their mechanical performance and suitability for the intended applications. The comprehensive data provided in the tables enable a detailed analysis of the components used throughout the study.

Table 2
Material specifications for composite layers.

Material composite	GEP	BEP	CEP
E_1 (Gpa)	50	208	155
E_2 (Gpa)	15.20	25.44	12.10
E_3 (Gpa)	15.20	25.44	12.10
G_{12} (Gpa)	4.70	7.24	4.40
G_{13} (Gpa)	4.70	7.24	4.40
G_{23} (Gpa)	3.28	4.9	3.20
V_{12}	0.254	0.1677	0.248
V_{13}	0.254	0.1677	0.248
V_{23}	0.428	0.36	0.458
ρ=Density kg/m^3	1900	2000	1600
X_t (Mpa)	1000	1300	1500
X_C (Mpa)	-600	-2000	-1250
Y_t (Mpa)	30	70	50
Y_C (Mpa)	-120	-300	-200
S (Mpa)	70	80	100

3.3. Boundary Conditions of the Problem

The boundary conditions and loading scenarios for the analyzed components in this study are defined as follows:

- The parts are subjected to loading exclusively in the X-direction. One edge of the part is fully constrained, restricting all degrees of freedom, while the opposite edge is allowed to move only in the direction of the applied load (X-direction). This setup effectively simulates a uniaxial loading condition.

- The applied load has a magnitude of 100 MPa and is gradually increased in a linear manner over a duration of one second. This controlled application ensures a realistic and stable loading scenario.

Fig. 9 illustrates the boundary conditions and loading configuration implemented in Abaqus. The fixed edge, the direction of the applied load, and the linear loading profile are clearly depicted, providing a complete visualization of the problem setup. Accurately defining these boundary conditions and loading parameters is essential for simulating the behavior of the composite components and obtaining reliable results from the finite element analysis.

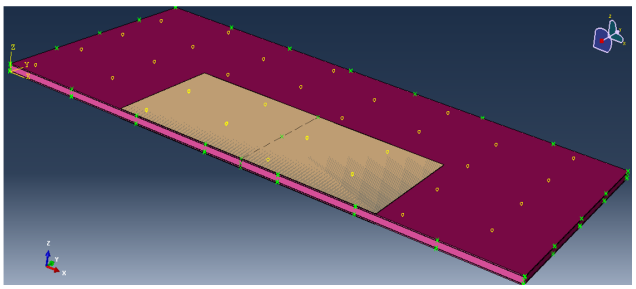

Fig. 9. Boundary conditions of the sample composite sheet.

4. Results and Discussion

4.1. Symmetry Effects in One-Sided and Two-Sided Patch Repairs

In one-sided patch repairs, the shift of the neutral axis causes the forces acting on the repaired region to be off-center. This generates significant torque at the connection, leading to curvature and bending of the repaired structure. Such bending is clearly observed in the patch application area and represents a key limitation of one-sided repair techniques (Fig. 10a, b).

In contrast, two-sided patch repairs provide a more symmetrical load transfer. Due to the balanced placement of patches on both sides, applied forces do not induce significant deformation along the Z-axis (Fig. 11a, b). This symmetric load distribution is a major advantage of the bilateral patch repair method, as it helps preserve the original shape and structural integrity of the repaired component.

4.2. Comparison of Stress and Strain at the Crack Location

To evaluate the effectiveness of the repair techniques, a tensile load of 100 MPa was applied in the X-direction over a duration of 1 second, distributed at equal intervals. This loading scenario enabled analysis of the strain development at the crack tip, as illustrated in the strain–time diagram (Fig. 12a).

The results indicate that the two-sided patch repair method is more effective at reducing stress (σ_x) over time compared to the one-sided repair. In particular, BEP patches applied bilaterally on the cracked structure exhibit the best performance in mitigating strain at the crack location. This enhanced strain reduction is attributed to the symmetric load transfer and uniform stress distribution provided by the two-sided patch configuration. The balanced repair minimizes stress concentrations at the crack tip, resulting in a more gradual and controlled strain development.

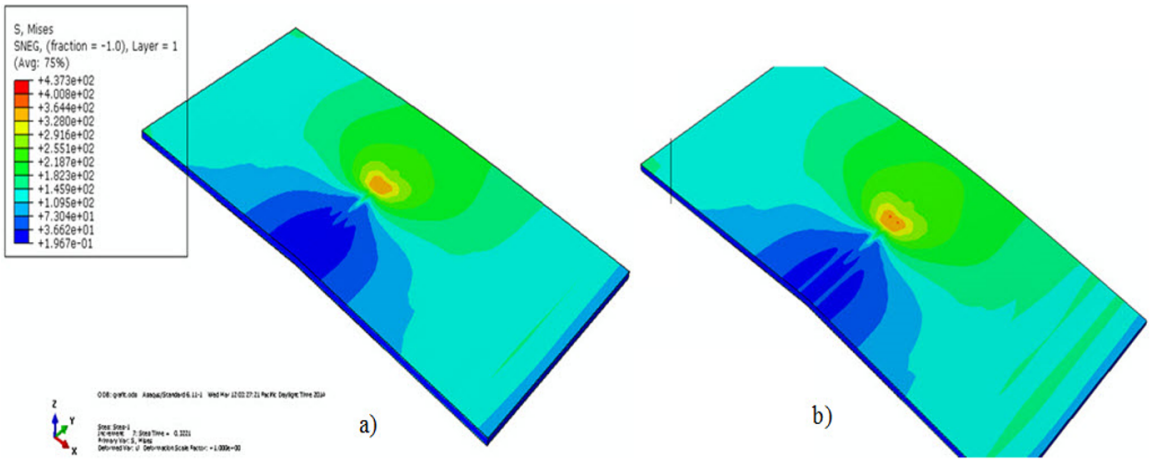

Fig. 10. One-sided patch repair using a) CEP patch, b) BEP patch.

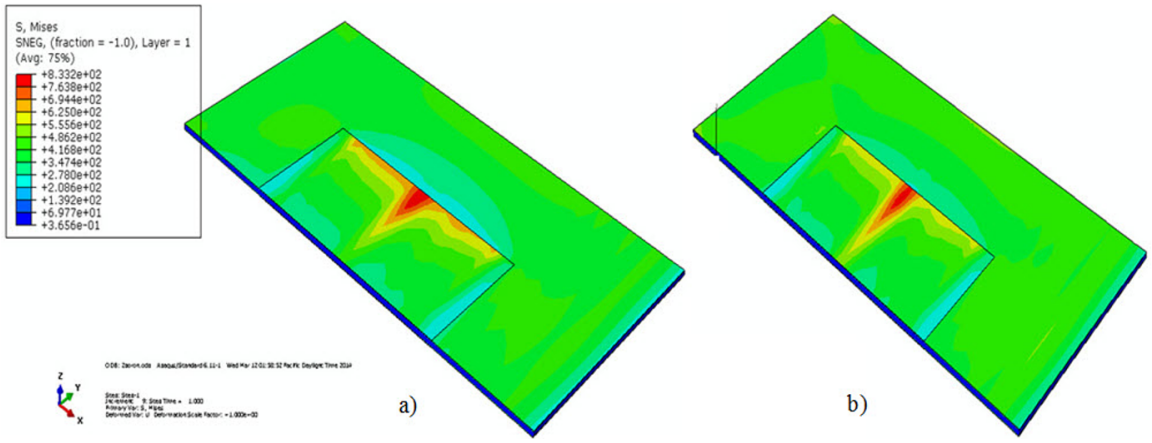

Fig. 11. Two-sided patch repair using a) CEP patch, b) BEP patch.

In contrast, the one-sided patch repair is less effective, as asymmetric load transfer leads to higher stress concentrations and more rapid strain accumulation at the crack tip. Consequently, the two-sided BEP patch emerges as the preferred approach for optimizing structural integrity and durability. Its symmetric load distribution, along with the elimination of Z-axis bending or deformations, helps preserve the original shape of the component, minimizes distortions, and ensures a more reliable restoration of the repaired structure's functionality.

Due to the superior performance of the two-sided patch repair, as evidenced by the reduced stress and strain at the crack location, this study further investigated the optimization of the composite patch design. Two optimization techniques-the Genetic Algorithm (GA) and the Imperialist Competitive Algorithm (ICA)-were employed to develop optimized patch configurations for the bilateral repair. The focus on two-sided patches was motivated by their key advantages, including the elimination of bending deformations and more effective mitigation of stress and strain at the crack. By applying these optimization algorithms, the study aimed to further enhance the performance and efficiency of the repair solution.

Following the incremental application of a 100 MPa tensile load over one second, the stress evolution at the crack tip was analyzed and is presented in the stress-time diagram (Fig. 12b). The results confirm that two-sided patch repairs are more effective at reducing crack-tip stress compared to one-sided repairs. Among the tested configurations, bilaterally applied boron-epoxy (BEP) patches demonstrated the highest stress mitigation performance, highlighting their suitability for optimizing structural integrity in repaired composite components.

The superior stress reduction achieved with the bilateral BEP patch repair is primarily due to the symmetric load transfer and the uniform distribution of stresses across the crack region. This balanced configuration effectively mitigates the stress concentrations that typically form at the crack tip, resulting in a more gradual and controlled stress buildup over time. In contrast, one-sided patch repairs are less effective, as asymmetric load transfer generates higher stress concentrations, leading to a faster and more pronounced increase in crack-tip stress.

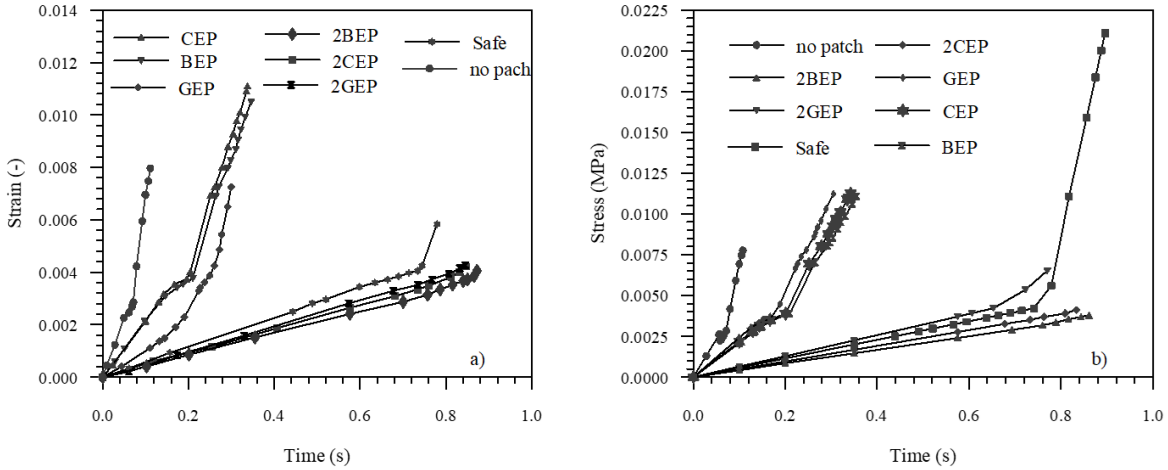

Fig. 12. a) Strain versus time, b) Stress versus time.

Consequently, the two-sided BEP patch emerges as the preferred approach for enhancing the structural integrity and durability of repaired components by minimizing the harmful effects of stress at the crack location. The stress analysis further underscores the advantages of the bilateral repair, particularly when employing the optimized BEP composite. This method offers significant improvements in stress management and overall structural performance, making it a highly effective solution for a wide range of engineering applications.

The stress and strain analysis of the damaged sheet, both without a patch and with one-sided and two-sided patches made of GEP and CEP, shows that double-sided patches can withstand higher stresses. Moreover, the stress response of the sheet repaired with two-sided patches closely approaches that of the undamaged sheet, indicating that this repair method effectively restores structural performance.

Optimization of the composite patches further reveals that BEP patches offer the highest stress tolerance at equivalent strain levels. This finding highlights the potential of BEP as the most suitable material for repairing the damaged sheet.

Fig. 13 presents the stress-strain relationship for the various repair configurations. This visual comparison clearly demonstrates the relative performance of different patch materials and configurations, providing insight into their effectiveness. Overall, the analysis indicates that two-sided patch repairs, particularly those using BEP composites, offer the most effective solution for restoring the damaged sheet, achieving the highest stress tolerance and the closest mechanical performance to the healthy, undamaged state.

4.3. Impact of Patch Layer Arrangement on Crack Opening Displacement

The arrangement of patch layers significantly influences the displacement at the crack opening, as shown in Fig. 14a. This figure illustrates how the crack length increases depending on the layer configuration within the applied patches on the sample. Fig. 14b presents the stress distribution along the crack length, providing valuable insight into how stresses are transferred and concentrated within the damaged area.

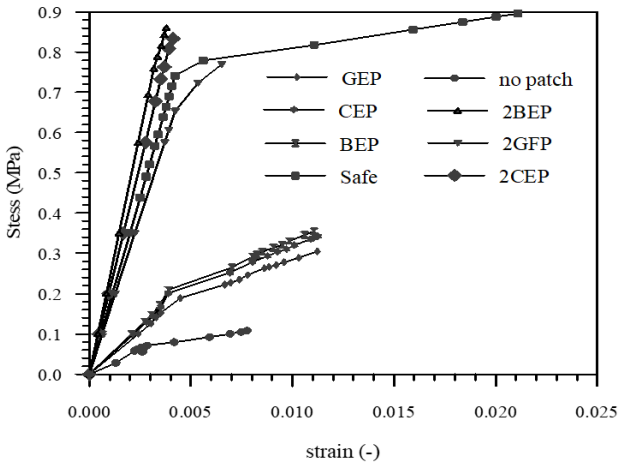

Fig. 13. Stress versus strain diagram.

Analysis of these results indicates that double-sided patches are more effective at reducing crack opening under higher stress levels. In particular, a bilaterally symmetric arrangement using a boron–epoxy (BEP) composite patch offers the most effective solution for minimizing both crack opening and stress concentration at the crack tip.

This finding highlights the importance of the strategic placement and configuration of patch layers in enhancing repair effectiveness. By optimizing the patch arrangement, crack opening can be effectively controlled, and stress concentrations at the crack tip can be reduced, resulting in a more robust and reliable repair. The visualizations in Figs. 14a and 14b offer a clear and detailed understanding of crack behavior and stress distribution, providing engineers and technicians with the insights needed to select the most effective repair strategy for the damaged structure.

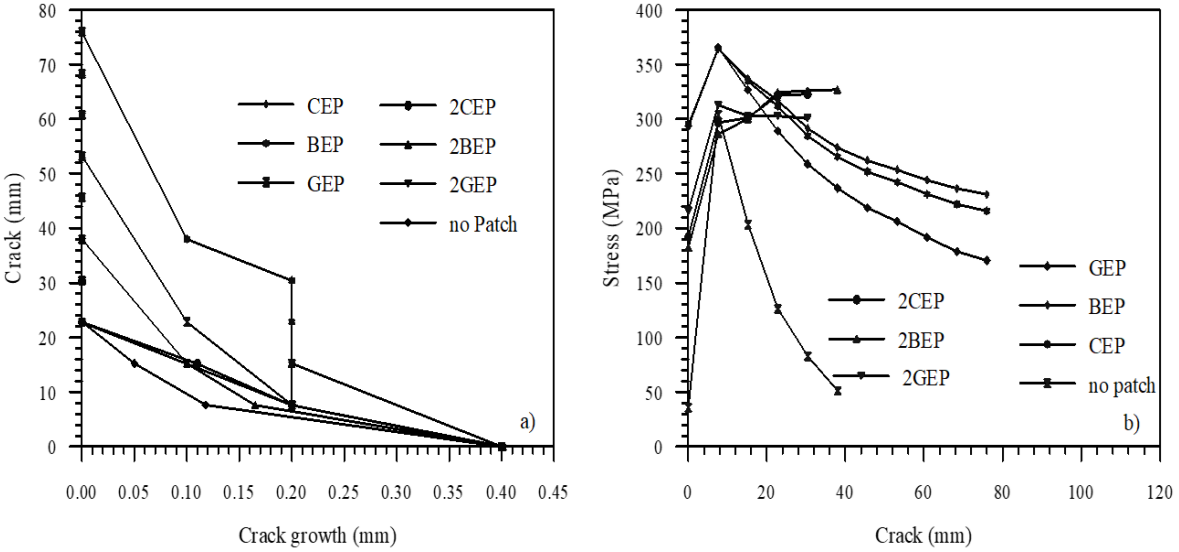

Fig. 14. a) Variation of crack width with crack length, b) Stress distribution along the crack length.

4.4. Optimization of the Problem

Under a tensile load of 100MPa applied in the X-direction over one second at equal intervals, the strain and stress at the crack tip in the tested samples are shown in Figs. 15a and 15b. The results indicate that bilateral patch repairs are more effective at reducing stress (σ_x) over a prolonged period. Among the tested materials, bilaterally applied boron-epoxy (BEP) patches provide the most significant reduction in strain at the crack tip.

Given the superior performance of bilateral patches and the absence of bending when using these configurations, the study further explored the use of optimized composite patches. Optimization was carried out using two computational methods: GA and ICA, both applied in a bilateral arrangement. These advanced optimization techniques enabled the refinement of patch designs, resulting in enhanced stress and strain reduction at the crack tip. By combining bilateral patch application with computational optimization, the overall effectiveness of the repair solution was significantly improved.

The GA and ICA optimizations were implemented using MATLAB, considering three key design parameters: layer material, fiber orientation, and layer thickness. Comparison of the results, presented in Table 3, shows that the ICA achieved higher optimization performance, with a superior value of the objective function and faster convergence to the optimal solution. Simulation results indicate that the ICA outperforms the GA in terms of response efficiency and optimality.

The patches obtained from both the GA and ICA optimizations were subsequently applied bilaterally in the sheet repair problem to evaluate their performance.

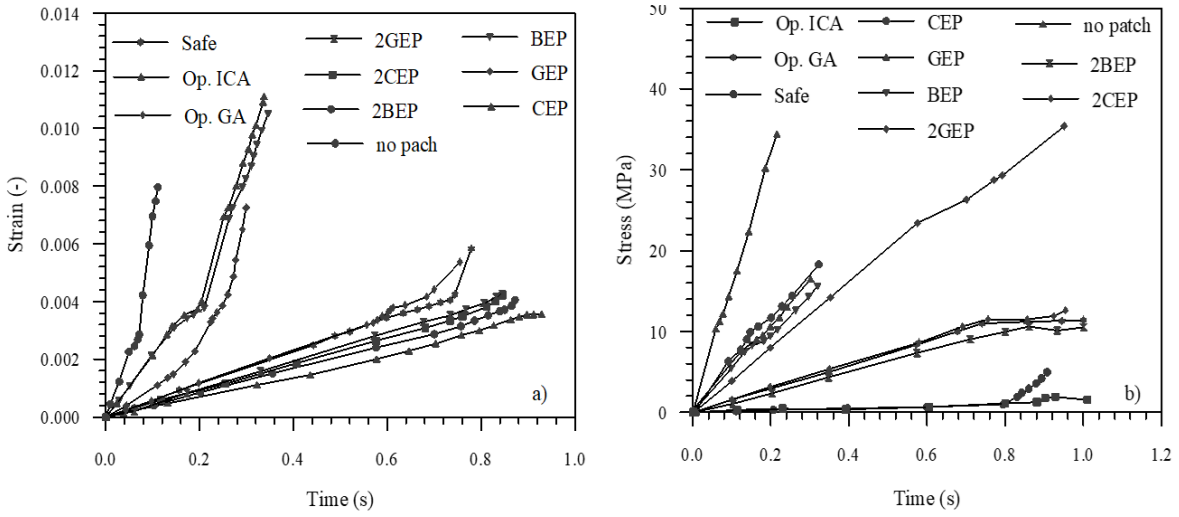

Fig. 15. a) Strain-time diagram and b) Stress–time diagram, including comparison with optimized patch designs.

Table 3
Results of optimization using the Genetic Algorithm and Imperialist Competitive Algorithm.

	Genetic Algorithm (GA)	Imperialism Competitive Algorithm (ICA)
Answers code	[5 7 11| 6 7 5 | 5 7 11 | 7 4 1]	[7 7 1| 6 7 1 | 7 7 1 | 5 11 1]
T(mm)	[0.175 | 0.175 | 0.175 | 0.1]	[0.175 | 0.175 | 0.175 | 0.275]
$\Theta(0)$	[-60 | 60 | -60 |0]	[0 | 0 | 0 |0]
Mat	[CEP | CEP | CEP | CEP]	[CEP | CEP | CEP | CEP]
W(kg)	0.0025	0.0061
C(t)	0.1520	0.1400
N_X(kg/m)	4.7243×10^4	3.8934×105
Fit.var	4.1308	4.2779

Fig. 16 presents the stress and strain analysis for the damaged sheet without a patch, the healthy sheet, and the repaired states using one-sided and two-sided patches made from different composite materials (GEP, CEP, and BEP). The figure also includes results from optimized patch configurations obtained using GA and ICA.

As illustrated, repairs with double-sided patches exhibit higher stress resistance compared to other configurations. Additionally, the stress tolerance of the double-sided patch repair closely approaches that of the undamaged sheet, indicating that this repair method effectively restores the structural performance of the component.

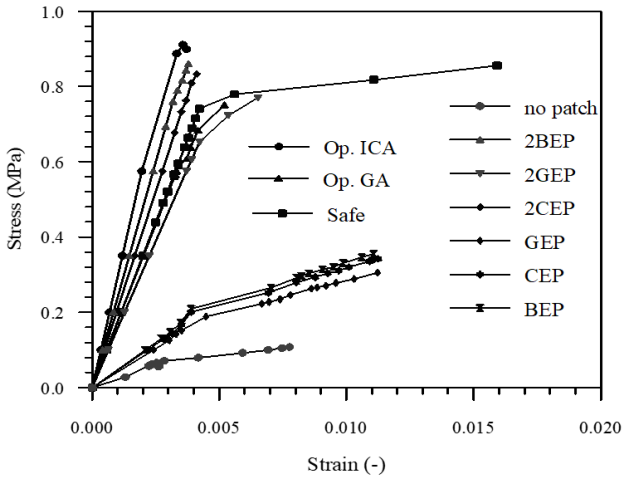

Fig. 16. Stress and strain comparison for different repair and material configurations.

The analysis of the optimized composite patches indicates that those optimized using the Imperialist Competitive Algorithm (ICA) exhibit the highest stress tolerance at equivalent strain levels. This finding suggests that ICA-optimized patches provide the most effective solution for repairing the damaged sheet, restoring its structural integrity close to that of the undamaged state. The use of advanced optimization techniques, such as the Genetic Algorithm (GA) and ICA, has enabled the identification of optimal repair designs. Among these, the two-sided ICA-optimized patch stands out for its ability to withstand higher stresses while maintaining a repaired state closely resembling the healthy sheet.

Composite patches were optimized using both GA and ICA methods, and the resulting designs were modeled and compared with previous repair configurations. As shown in Fig. 17, ICA-optimized patches significantly reduce crack growth and increase the rupture load. Double-sided patches, in particular, are more effective at limiting crack opening under higher stress levels, with the ICA-optimized configuration providing the best overall performance.

The superior performance of ICA-optimized patches in controlling crack growth and enhancing rupture load can be attributed to the algorithm's efficient exploration of the design space and its ability to converge to a global optimum. In contrast, GA-optimized patches, while improving performance, do not achieve the same level of crack mitigation or load-bearing capacity as ICA-optimized patches. This highlights the critical role of selecting an appropriate optimization technique for a given problem, with ICA demonstrating clear advantages in this application.

Overall, the results presented in Fig. 17 demonstrate the effectiveness of ICA-optimized composite patches in enhancing the structural integrity of damaged components. These findings provide valuable guidance for engineers and researchers in the design and optimization of composite repair solutions across a range of practical applications.

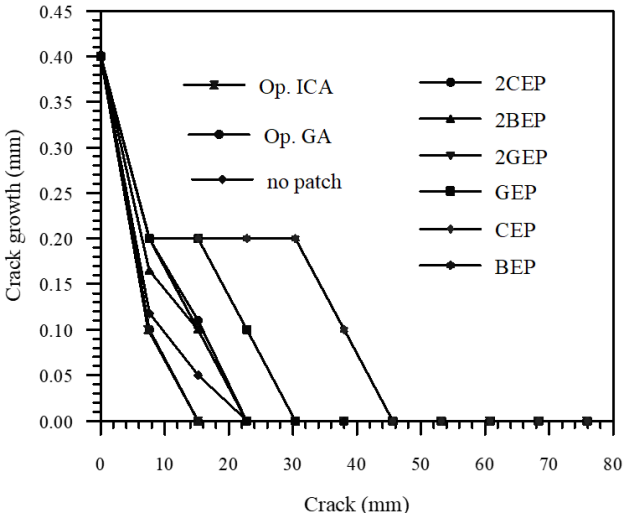

Fig. 17. Crack width along increasing crack length.

5. Conclusion

This study investigated the effectiveness of composite patch repairs in mitigating crack growth in damaged composite sheets using a combined finite element analysis (FEA) and optimization approach. Three repair configurations were analyzed: unrepaired, one-sided patch, and symmetric two-sided patch. A multi-objective optimization framework was developed using the Genetic Algorithm (GA) and the Imperialism Competitive Algorithm (ICA) to identify optimal patch designs balancing weight, cost, and structural performance. The key findings of this research are summarized as follows:

- Effectiveness of Composite Patch Repairs: The symmetric two-sided composite patch significantly reduced crack-tip stress, strain, and strain energy release rate (SERR) compared to the unrepaired and one-sided patch configurations. One-sided patches improved structural performance but introduced bending and asymmetric deformation, reducing overall repair efficiency.
- Optimization Outcomes: The optimization framework successfully identified patch designs that minimized weight and cost while maximizing load-carrying capacity. The ICA consistently outperformed the GA by providing superior convergence, lighter and more cost-effective designs, and higher structural performance.
- Practical Implications: Symmetric two-sided patches, combined with optimized layer orientations and material selection, offer the most efficient and reliable repair solution for damaged composite sheets. Integration of FEA with multi-objective optimization provides a powerful tool for designing lightweight, cost-effective, and high-performance composite repairs.

This study provides comprehensive insights into crack mitigation strategies and the influence of patch design on composite sheet performance. Future research may extend the framework to consider fatigue loading, impact damage, environmental effects, and more complex geometries to further enhance repair strategies for real-world applications. In conclusion, the combination of symmetric composite patch repair and optimization-based design represents a robust, cost-efficient, and practical solution for extending the service life of damaged composite structures, offering valuable guidance for engineers in aerospace, automotive, and other advanced engineering applications.

References

[1] F. Khan, N. Hossain, J. J. Mim, S. M. Rahman, M. J. Iqbal, M. Billah, M. A. Chowdhury. Advances of composite materials in automobile applications-A review, J. Eng. Res., 13(2) (2025) 1001.

[2] L. Gabrehiwet, E. Abate, Y. Negussie, et al.. Application of Composite Materials in Aerospace: A review, Int. j. adv. eng. manag. res., 5(3) (2023) 697.

[3] D. ouinas, B. Bouiadjra, S. Himouri. Progressive edge cracked aluminum plate repaired with adhesively bonded composite patch under full width disband, composite, Comput. Mater. Sci., 43(13) (2012) 805-811.

[4] A. Aabid, M. Hrairi, J. Mohammad Ali, et al.. A Review on Reductions in the Stress-Intensity Factor of Cracked Plates Using Bonded Composite Patches, Composites Materials for Aeronautical Structural Application, 15(9) (2023) 3086.

[5] L. Echer, O. Ochoa, C. E. Souza, R. J. Marczak. A modal-based shape optimization methodology for conventionally shaped patches in composite plate repair, Compos. Part B Eng., 309 (2026) 113084.

[6] R. E. Philip, A. D. Andrushia, A. Nammalvar, et al.. A Comparative Study on Crack Detection in Concrete Walls Using Transfer Learning Techniques, J. Compos. Sci., 7(4) (2023) 169.

[7] A. Maleki, , M. Saeedifar, et al.. The fatigue failure study of repaired aluminum plates by composite patches using acoustic mission, Eng. Fract. Mech., 210 (2019) 300-311.

[8] M. A. Bellali, B. Serier, M. Mokhtari, et al.. XFEM and CZM modeling to predict the repair damage by composite patch of aircraft structures: Debonding parameters, Compos. Struct., 266 (2021) 113805.

[9] S. M. K. Mohammed, R. Mhamdia, A. Albedah, et al.. Fatigue crack growth in aluminum plates repaired with different shapes of single-sided composite patches. Int. J. Adhes. Adhes., 105 (2021) 102781.

[10] H. Zarrinzadeh, M. Z. Kabir, A. Deylami. Extended finite element fracture analysis of a cracked isotropic shell repaired by composite patch, Fatigue Fract. Eng. Mater. Struct., 39(11) (2016) 1352-1365.

[11] L. Ke, C. Li, J. He, et al.. Enhancing fatigue performance of damaged metallic structures by bonded CFRP patches considering temperature effects, Mater. Des., 192 (2020) 108731.

[12] A. Aabid, Y. E. Ibrahim, M. Hrairi, J.S.M. Ali. Optimization of Structural Damage Repair with Single and Double-Sided Composite Patches through the Finite Element Analysis and Taguchi Method, Materials, 16 (2023) 1581.

[13] H. Zarrinzadeh, M. Z. Kabir, A. Deylami. Extended finite element fracture analysis of a cracked isotropic shell repaired by composite patch, Fatigue Fract. Eng. Mater. Struct., 39(11) (2016) 1352.

[14] M. Abdolahi, A. Isazadeh, D. Abdolahi. Imperialist Competitive Algorithm for Solving Systems of Nonlinear Equations, Comput. Math. Appl., 65(12) (2013) 1894.

[15] H. D. Mazraeh, K. Parand, H. Farahani, et al.. An improved imperialist competitive algorithm for solving an inverse form of the Huxley equation, Iran. J. Numer. Anal. Optim., 14(3) (2024) 681.

[16] T. Otani, W. Sumihira, Y. Kobayashi, M. Tanaka. Density-based topology optimization of thin plate structure with geometric nonlinearity using a three-dimensional correlational triangle element formulation, Struct. Multidiscip. Optim., 65 (2022) 282.

[17] S. Şimşek, V. Kahya, G. Adıyaman, V. Toğan. Damage detection in anisotropic-laminated composite beams based on incomplete modal data and teaching-learning-based optimization, Struct. Multidiscip. Optim., 65 (2022) 332.

[18] X. Liu, Y. He, D. Qiu, Z. Yu. Numerical optimizing and experimental evaluation of stepwise rapid high-pressure microwave curing carbon fiber/epoxy composite repair patch, Compos. Struct., 230 (2019) 111529.

[19] M. Masoudpour, A. Bagheri, M. J. Mahmoodabadi. Using a New Strategy in Imperialist Competitive Algorithm to Solve Multi-objective Problems, J. Algorithm Comput., 14(3) (2024) 681.